

# Impact of $J/\psi$ pair production at the LHC and predictions in nonrelativistic QCD

Li-Ping Sun<sup>a,\*</sup>, Hao Han<sup>a,†</sup> and Kuang-Ta Chao<sup>a,b,c,‡</sup>

(a) School of Physics and State Key Laboratory of Nuclear Physics and Technology, Peking University, Beijing 100871, China

(b) Collaborative Innovation Center of Quantum Matter, Beijing, China

(c) Center for High Energy physics, Peking University, Beijing 100871, China

For  $J/\psi$  pair production at hadron colliders, we present the full next-to-leading order (NLO) calculations in nonrelativistic QCD (NRQCD). We find that the NLO result can reasonably well describe the LHCb cross section, but exhibits very different behaviors from the CMS data in the transverse momentum distribution and mass distribution of  $J/\psi$  pair. Moreover, adding contributions of gluon and quark fragmentation is found to be unable to reduce the big differences. In particular, the observed flat distribution in the large invariant mass is hard to understand. NRQCD may face a challenge if this  $J/\psi$  pair experiment is confirmed.

PACS numbers: 12.38.Bx, 13.60.Le, 14.40.Pq

*Introduction.*—Nonrelativistic QCD (NRQCD)[1] is now widely accepted in the study of heavy quarkonium physics. In NRQCD a quarkonium production process can be factorized as short distance coefficients and long distance NRQCD matrix elements (LDMEs). This factorization has been applied in single quarkonium production and its validity has been tested by various experiments[2–7].

Besides the single quarkonium production, the multi-quarkonium production provides another ideal laboratory to understand the quarkonium production mechanism that NRQCD assumes. At the LHC, the LHCb Collaboration in 2011 measured the  $J/\psi$  pair production for the first time at the center-of-mass energy  $\sqrt{s} = 7$  TeV with an integrated luminosity of  $35.2 \text{ pb}^{-1}$ [8]. Very recently, the CMS Collaboration further released the preliminary data of  $J/\psi$  pair production[9] with a much larger  $p_T$  range, providing a good platform for testing the validity of NRQCD in quarkonium pair production.

In Refs.[10–12], the leading order (LO) calculation of  $J/\psi$  pair production in the color singlet model (CSM) is performed. The relativistic correction to the  $J/\psi$  pair production is carried out [13], where the relativistic correction makes significant improvement for diluting the discrepancy between the shape of color-singlet (CS) differential cross sections and that of the color-octet (CO) at LO. Besides, the partial next-to-leading order (NLO\*) correction for  $J/\psi$  pair production is evaluated by Lansberg and Shao [14], where they consider that at large  $p_T$  the NLO\* yield can completely reproduce the full NLO result, and their NLO\* results give a more precise theoretical prediction compared to the LO one. All the above works are performed in the single parton scattering (SPS) model, while the contribution of double parton

scattering (DPS) is assessed in Refs.[15–17]. In Ref.[15] a crystal ball function is introduced for parameterizing the  $J/\psi$  pair production matrix element, which separates the small  $p_T$  contribution from the higher one, and improves the LO SPS prediction significantly.

In order to further understand the multi-quarkonium production mechanism, it is necessary to evaluate the  $J/\psi$  pair production at NLO in NRQCD. Compared to the LO calculation, the NLO calculation can decrease the uncertainties and make more precise predictions. So in this work, the full NLO calculation for  $J/\psi$  pair production in SPS at the LHC is evaluated. For the LHCb, we will give the transverse momentum distribution, and make a comparison between NLO and NLO\* yield. While for the CMS, fixed order NRQCD calculation can be used properly with a small  $p_T$  cutoff. Therefore, this work mainly focuses on the new data measured by the CMS.

*Formalism.*—In NRQCD, the cross section of  $J/\psi$  pair production at the LHC can be expressed as

$$d\sigma = \sum_{i,j,n} \int dx_1 dx_2 f_{i/p}(x_1) f_{j/p}(x_2) \langle \mathcal{O}_n \rangle \langle \mathcal{O}_n \rangle d\hat{\sigma}^{i,j,n}. \quad (1)$$

where  $f_{i/p}(x_{1,2})$  is the parton distribution function (PDF), and  $x_i$  represents the momentum fraction of the partons from the proton,  $\langle \mathcal{O}_n \rangle$  are the LDMEs with  $n = {}^3S_1^{[1]}$  in our NLO calculation,  $d\hat{\sigma}$  is the short distance coefficient, which can be computed by using the covariant projection operator method, for  $J/\psi({}^3S_1)$ , we employ the following commonly used projection operators for spin and color:

$$\Pi_1 = \frac{1}{\sqrt{8m_c^3}} \left( \frac{P}{2} - m_c \right) \not{\epsilon}_{J/\psi} \left( \frac{P}{2} + m_c \right). \quad (2)$$

and

$$\mathcal{C}_1 = \frac{1}{\sqrt{N_c}}. \quad (3)$$

where  $\epsilon_{J/\psi}^\mu$  is the  $J/\psi$  polarization vector with  $P \cdot \epsilon = 0$ ,  $P$  is the momentum of  $J/\psi$ .

\*Electronic address: sunliping@pku.edu.cn

†Electronic address: hao.han@pku.edu.cn

‡Electronic address: ktchao@pku.edu.cn

In the LO calculation, there are two subprocesses:  $g + g \rightarrow J/\psi + J/\psi$  and  $q + \bar{q} \rightarrow J/\psi + J/\psi$ , only the former is taken into account since the contribution of the other process is negligible. While in the NLO case, besides the gluon fusion process, the quark gluon process  $q + g \rightarrow 2J/\psi + q$  should also be considered. To tackle the infra-red (IR) divergences in real corrections at NLO, the two-cut-off phase space slicing method[18] is introduced, the soft divergences and collinear divergences are well isolated. Finally the cross sections for the  $J/\psi$  pair production at the NLO can be expressed as

$$\sigma_{NLO} = \sigma_{Born} + \sigma_{Virtual} + \sigma_{Real}^{soft} + \sigma_{Real}^{HC} + \sigma_{Real}^{\overline{HC}}, \quad (4)$$

where  $HC$  and  $\overline{HC}$  represent hard collinear and hard non-collinear contributions, respectively.

It is known that at large transverse momentum, the quarkonium production is dominated by parton fragmentation, so we should take these contributions into account. For double  $J/\psi$  production, the quark and gluon fragmentation processes can be expressed as

$$d\sigma_{A+B \rightarrow 2J/\psi + X} = \sum_{ijn_1n_2} d\hat{\sigma}_{A+B \rightarrow i+j+X} \otimes D_{i \rightarrow Q\bar{Q}(n_1)} \otimes D_{j \rightarrow Q\bar{Q}(n_2)}, \quad (5)$$

where  $D_{i,j \rightarrow Q\bar{Q}(n_1,n_2)}$  are the single-parton fragmentation functions (FFs). In our calculation, up to NLO in  $\alpha_s$ , all the possible fragmentation channels  $i = j = g, n_1 = n_2 = {}^3S_1^{[8]}, {}^1S_0^{[8]}, {}^3P_J^{[8]}$  and  $i = c, j = \bar{c}, n_1 = n_2 = {}^3S_1^{[1]}, {}^3S_1^{[8]}, {}^1S_0^{[8]}, {}^3P_J^{[8]}$  are taken into account, and the expressions of these FFs can be found in Ref.[19]. The FFs are scale dependent, and the large logarithms of  $\mu_f^2/(2m_c)^2$  are summed up by using the DGLAP evolution equation [20–24]

$$\frac{d}{d \log \mu_f^2} \begin{pmatrix} D_c \\ D_g \end{pmatrix} = \frac{\alpha_s(\mu_f)}{2\pi} \begin{pmatrix} P_{cc} & P_{gc} \\ P_{cg} & P_{gg} \end{pmatrix} \otimes \begin{pmatrix} D_c \\ D_g \end{pmatrix}, \quad (6)$$

where  $D_g$  and  $D_c$  denote the FFs of gluon fragmentation and charm quark fragmentation, respectively,  $P_{ij}$ s are the DGLAP splitting functions for FFs.

**Numerical Inputs.**—Because of the complexity of the  $J/\psi$  pair production, in our calculation, the computer algebra system MATHEMATICA is employed with the help of the package FEYNARTS [25] to generate the Feynman diagrams and amplitudes. The phase space integration is evaluated by employing the package LoopTools and Vegas.

In numerical calculation, the CTEQ6L1 and CTEQ6M are used for the parton distributions[26, 27]. Specifically, the renormalization scale  $\mu_r$  and factorization scale  $\mu_f$  are chosen as  $\mu_r = \mu_f = m_T$ , with  $m_T = \sqrt{p_T^2 + 16m_c^2}$ . In the two cutoff method,  $\delta_s$  and  $\delta_c$  are set to be  $\delta_s = 10^{-3}$ ,  $\delta_c = 10^{-5}$ . The uncertainties are estimated by varying  $\mu_r$  and  $\mu_f$  from  $m_T/2$  to  $2m_T$  and choosing  $m_c = 1.55 \pm 0.05$  GeV.

In the  $J/\psi$  pair production, the  ${}^3S_1^{[1]}$  LDME can be estimated by the B – T potential model[28], and the  ${}^1S_0^{[8]}$ ,  ${}^3S_1^{[8]}$  and  ${}^3P_0^{[8]}$  LDMEs can be taken from Ref. [29], and given in Tab. I.

$\langle \mathcal{O}({}^3S_1^{[1]}) \rangle$	$\langle \mathcal{O}({}^3S_1^{[8]}) \rangle$	$\langle \mathcal{O}({}^1S_0^{[8]}) \rangle$	$\langle \mathcal{O}({}^3P_0^{[8]}) \rangle / m_c^2$
GeV <sup>3</sup>	10 <sup>-2</sup> GeV <sup>3</sup>	10 <sup>-2</sup> GeV <sup>3</sup>	10 <sup>-2</sup> GeV <sup>3</sup>
1.16	0.3	8.9	0.56

TABLE I: The LDMEs for  $J/\psi$  pair production. The CS LDME is estimated by the B – T potential model in Ref.[28] and the CO LDMEs are taken from Ref. [29].

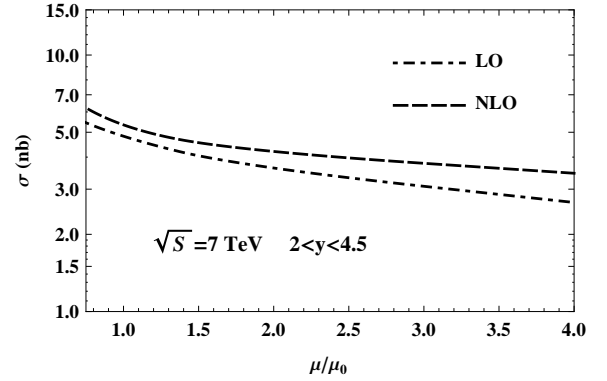


FIG. 1: The scale dependence of total cross sections for LO and NLO at LHCb. The dashed line and dash-dotted line represent the NLO and LO results, respectively. Here  $\mu_0 = m_T$  and the scale  $\mu = \mu_r = \mu_f$  varies from  $3/4\mu_0$  to  $4\mu_0$ .

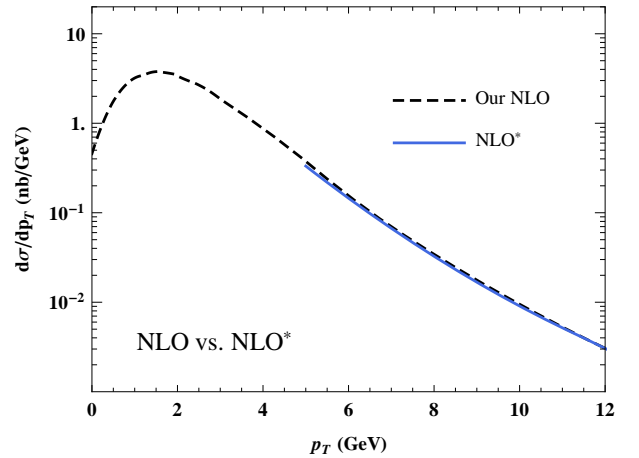


FIG. 2: (color online). Comparison between full NLO and NLO\* results of  $p_T$  distribution in  $J/\psi$  pair production at LHCb. The solid line and dash-dotted line denote the NLO\* and NLO results, respectively. The same charm quark mass  $m_c = 1.5$  GeV is chosen as in Ref.[14].

**Results.**—At the LHCb with  $\sqrt{S} = 7$  TeV,  $2 < y(J/\psi) < 4.5$ ,  $0 < p_T < 10$  GeV [8], the calculated

central values of cross sections at LO and NLO (with  $\mu_r = \mu_f = m_T$ ,  $m_c = 1.55$  GeV) are  $\sigma_{\text{LO}} = 4.83$  nb,  $\sigma_{\text{NLO}} = 5.34$  nb, which are compatible with the LHCb measured value  $\sigma^{J/\psi J/\psi} = 5.1 \pm 1.0 \pm 1.1$  nb. In addition, the scale dependence is evaluated, which is an important criterion for the NLO calculation. As shown in Fig.1, the scale dependence at NLO is obviously weakened compared to that at LO. This reduces the uncertainties due to scale choice and makes the NLO predictions more accurate and reliable. Furthermore, we compare our full NLO  $p_T$  distribution with the NLO\* one in Ref. [14], which is shown in Fig. 2. It is interesting to note that when  $p_T > 6$  GeV the full NLO  $p_T$  distribution is consistent with the NLO\* one. That is, the NLO\* can accurately reproduce the full NLO yield at moderate and large  $p_T$  [14]. However, it should be worthwhile to point out their differences here. First, although the NLO\* calculation can well describe the large  $p_T$  behavior, it is not a complete calculation. The infrared cuts  $s_{ij}$  must be introduced to regulate the infrared (IR) divergence. In the region  $p_T > 5$  GeV, the  $s_{ij}$  dependence is weak. But when  $p_T < 5$  GeV the dependence increases [14]. So the NLO\* yield is IR cut related at small  $p_T$ , while the full NLO calculation exhibits no IR singularity in the whole  $p_T$  region. Second, because of the incompleteness, the NLO\* calculation may not give a good scale dependence, while the full NLO calculation can, as shown in Fig.1. Third, the full NLO calculation can give a relatively good description for the small  $p_T$  behavior, while the NLO\* cannot present a precise prediction owing to the increasing  $s_{ij}$  dependence. This difference is shown in Fig.2.

In the CMS conditions [9]:

$$\begin{aligned} &|y(J/\psi)| < 1.2 \text{ for } p_T > 6.5 \text{ GeV, or} \\ &1.2 < |y(J/\psi)| < 1.43 \text{ for } p_T > 6.5 \rightarrow 4.5 \text{ GeV, or} \\ &1.43 < |y(J/\psi)| < 2.2 \text{ for } p_T > 4.5 \text{ GeV,} \end{aligned}$$

the total cross section is measured to be

$$\sigma_{\text{Exp.}} = 1.49 \pm 0.07 \pm 0.14 \text{ nb.} \quad (7)$$

Under conditions of the CMS experiment, we calculate the LO and NLO total cross section:

$$\sigma_{\text{LO}} = 0.08 \pm 0.02 \text{ nb,} \quad \sigma_{\text{NLO}} = 0.98 \pm 0.16 \text{ nb.} \quad (8)$$

In (8), the contribution of feeddown process  $p + p \rightarrow J/\psi + \psi(2S) + X \rightarrow 2J/\psi + X$  is also included, which is estimated to be 30% of the direct process[12]. Comparing with (7) and (8), we find that the theoretical result is not consistent with the experimental data.

Meanwhile, we compare our prediction for the transverse momentum  $p_{TJ/\psi J/\psi}$  distribution of  $J/\psi$  pair, with both the NLO and fragmentation processes taken into account. The result is shown in Fig. 3. At LO,  $p_{TJ/\psi J/\psi}$  is always zero, because it is a two-body final state process. At NLO, unfortunately, as indicated in Fig. 3, the NLO result can not account for the CMS data either. The

behaviors are very different between the NLO prediction and the CMS data, and the NLO result exhibits a peak at much smaller  $p_{TJ/\psi J/\psi}$  than the CMS data. In addition, the fragmentation processes including all relevant channels contribute little to the  $p_{TJ/\psi J/\psi}$  distribution, and the gap between NLO result and CMS data cannot be decreased by these fragmentation contributions.

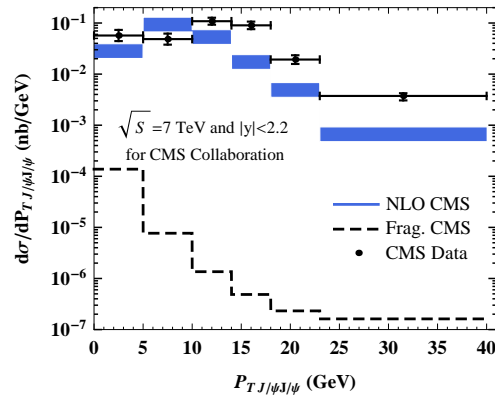


FIG. 3: (color online). Differential cross section in bins of the transverse momentum of  $J/\psi$  pair at CMS. The data are taken from Ref. [9]. The blue band denotes the NLO results, where the uncertainties are due to scale and charm quark mass choices as mentioned in the text, and the dashed line represents the fragmentation contributions including all relevant channels.

By integrating out the total cross section in different regions of  $J/\psi$  pair invariant mass, we can obtain the invariant mass distribution at CMS, which is shown in Fig. 4. We see that the NLO result can well describe the first two bins, but it begins to decrease rapidly from the third bin, indicating that the NLO behavior is very different from the CMS data: the latter is almost flat at large invariant mass, and larger than the NLO result by, surprisingly, several orders of magnitude. In fact, when  $M_{J/\psi J/\psi} > 22$  GeV, the NLO prediction is less than CMS data by almost two orders of magnitude, and when  $M_{J/\psi J/\psi} > 35$  GeV, the discrepancy raises to almost four orders of magnitude.

Intuitively, by examining the discrepancy in the  $J/\psi$  pair mass distribution, a large angle  $J/\psi$  pair production process is apparently needed. We then evaluate the quark and gluon fragmentation processes including all relevant channels. The total contribution of all fragmentation channels is shown in Fig. 4. Unfortunately, the fragmentation processes contribute little to the  $J/\psi$  pair production, thus the discrepancy between NLO result and CMS data can not be resolved by these processes, either.

We also consider other possible sources for the discrepancy, e.g., the  $Z^0$  boson decays to a  $J/\psi$  pair:  $Z^0 \rightarrow 2J/\psi + X$ . Under the CMS condition, the total cross section of this process is:  $\sigma = 2.5 \times 10^{-4}$  nb. Its contributions to each bin of the  $J/\psi$  pair transverse

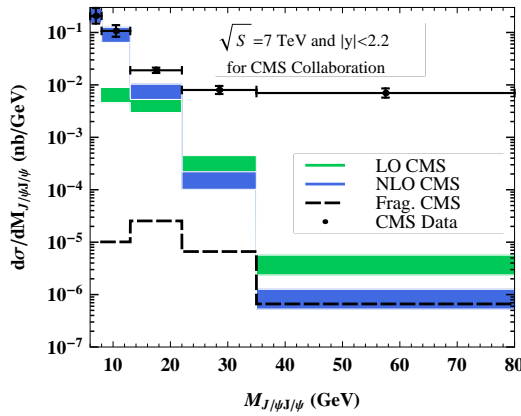


FIG. 4: (color online). Differential cross section in bins of the  $J/\psi$  pair invariant mass at CMS. The data are taken from Ref. [9]. The green and blue bands denote the LO and NLO theoretical results respectively, where the uncertainties are due to scale and charm quark mass choices as mentioned in the text. The dashed line represents the sum of the quark and gluon fragmentation from all relevant channels.

momentum distribution and invariant mass distribution, are of negligibly small values. So it is clear that with other possible processes contributing to the large angle production of the  $J/\psi$  pair, the big gap between theoretical predictions and CMS data still remains.

The discrepancies of total cross section,  $p_{TJ/\psi J/\psi}$  distribution, and invariant mass distribution between the NLO results and the CMS data, are attributed to the fact that at large  $p_T$  the NLO results demonstrate a  $p_T^{-6}$  behavior, while the CMS data behaves much flatter. Other

possible processes including fragmentation and  $Z^0$  decays cannot provide a sizable contribution to the large angle production of the  $J/\psi$  pair.

*Summary.*—In the framework of NRQCD, we evaluate the full NLO  $J/\psi$  pair production in the CSM model and also consider other possible processes for the large angle production of  $J/\psi$  pair including gluon and quark fragmentation and  $Z^0$  decays. At the LHCb, the comparison between our full NLO and NLO\* results demonstrates that the latter agree with the NLO results when  $p_T > 6$  GeV. In addition, our NLO calculation can give a reasonable description for the total cross section (including the small  $p_T$  region contribution) observed at LHCb. For the CMS, however, our predicted  $p_{TJ/\psi J/\psi}$  distribution and invariant mass distribution of  $J/\psi$  pair at NLO are very different from the CMS data. By taking other processes including gluon and quark fragmentation and  $Z^0$  decays into account, we find the discrepancies still remain. In particular, for the  $J/\psi$  pair invariant mass distribution, the observed flatness and orders of magnitude differences from theoretical predictions in the large invariant mass region ( $22 \text{ GeV} < M_{J/\psi J/\psi} < 80 \text{ GeV}$ ) are hard to understand in NRQCD. Contributions of higher order corrections and other possible processes are unlikely to be able to resolve the problem. If confirmed, this CMS measurement will be a challenge to NRQCD, and may even indicate the existence of some new mechanisms or phenomena. Further experimental and theoretical investigations are needed to clarify this issue.

We thank Y. Q. Ma, C. Meng, H. S. Shao, and Y. J. Zhang for valuable discussions and suggestions. This work was supported in part by the National Natural Science Foundation of China (No 11075002, No 11021092).

- 
- [1] G. T. Bodwin, E. Braaten, and G. P. Lepage, Phys. Rev. D **51**, 1125(1995).
  - [2] M. Butenschoen, and B. A. Kniehl, AIP Conf. Proc. **1343**, 409 (2011); M. Butenschoen, and B. A. Kniehl, Phys. Rev. Lett. **107**, 232001 (2011); M. Butenschoen, and B. A. Kniehl, Phys. Rev. Lett. **108**, 172002 (2012).
  - [3] M. Butenschoen, and B. A. Kniehl, Nucl. Phys. Proc. Suppl. **222**, 151 (2012); M. Butenschoen, and B. A. Kniehl, Mod. Phys. Lett. A **28**, 1350027 (2013); M. Butenschoen, Z. G. He and B. A. Kniehl, Phys. Rev. D **88**, 011501 (2013); B. A. Kniehl, and M. Butenschoen, PoS ICHEP2012, **278** (2013).
  - [4] Y. Fan, Y. Q. Ma and K. T. Chao, Phys. Rev. D **79**, 114009 (2009); Y. J. Zhang, Y. Q. Ma, K. Wang and K. T. Chao, Phys. Rev. D **81**, 034015 (2010); Y. Q. Ma, K. Wang and K. T. Chao, Phys. Rev. D **83**, 111503 (2011).
  - [5] Z. G. He, Y. Fan and K. T. Chao, Phys. Rev. D **75**, 074011 (2007); Y. Q. Ma, K. Wang and K. T. Chao, Phys. Rev. Lett. **106**, 042002 (2011); Y. Q. Ma, K. Wang and K. T. Chao, Phys. Rev. D **84**, 114001 (2011).
  - [6] B. Gong, and J. X. Wang, Phys. Rev. Lett. **100**, 232001 (2008); B. Gong, and J. X. Wang, Phys. Rev. D **78**, 074011 (2008); B. Gong, X. Q. Li and J. X. Wang, Phys. Lett. B **673**, 197 (2009).
  - [7] R. Li, and J. X. Wang, Phys. Lett. B **672**, 51 (2009); B. Gong, and J. X. Wang, Phys. Rev. D **83**, 114021 (2011); B. Gong, L. P. Wan, J. X. Wang and H. F. Zhang, Phys. Rev. Lett. **110**, 042002 (2013); B. Gong, L. P. Wan, J. X. Wang and H. F. Zhang, Phys. Rev. Lett. **112**, 032001 (2014).
  - [8] **LHCb Collaboration**, R. Aaij *et al.*, Phys. Lett. B **707**, 52 (2012).
  - [9] CMS Physics Analysis Summary, CMS PAS BPH-11-021, 2013.
  - [10] R. Li, Y. J. Zhang and K. T. Chao, Phys. Rev. D **80**, 014020 (2009).
  - [11] C. F. Qiao, L. P. Sun and P. Sun, J. Phys. G **37**, 075019 (2010).
  - [12] A. V. Berezhnoy, A. K. Likhoded, A. V. Luchinsky and A. A. Novoselov, Phys. Rev. D **84**, 094023 (2011).
  - [13] Y. J. Li, G. Z. Xu, K. Y. Liu and Y. J. Zhang, J. High Energy Phys. 1307 051 (2013).
  - [14] J. P. Lansberg and H. S. Shao, Phys. Rev. Lett. **111**, 122001 (2013).
  - [15] C. H. Com, A. Kulesza and W. J. Stirling, Phys. Rev. Lett. **107**, 082002 (2011).

- [16] D. d'Enterria and A. M. Snigirev, arXiv:1301.5845.
- [17] S. Baranov, A. Snigirev, and N. Zotov, Phys. Lett. B **705**, 116 (2011).
- [18] B. W. Harris and J. F. Owens, Phys. Rev. D **65** 094032 (2002).
- [19] Y. Q. Ma, J. W. Qiu, and H. Zhang, arXiv:1311.7078.
- [20] V. N. Gribov and L. N. Lipatov, Sov. J. Nucl. Phys. **15**, 438 (1972).
- [21] L. N. Lipatov, Sov. J. Nucl. Phys. **20**, 94 (1975).
- [22] Y. L. Dokshitzer, Sov. Phys. JETP **46**, 641 (1977).
- [23] G. Altarelli and G. Parisi, Nucl. Phys. B **126**, 298 (1977).
- [24] J. Pumplin, D.R. Stump, J. Huston, H. L. Lai, P. M. Nadolsky, and W. K. Tung, JHEP **0207**, 012 (2002).
- [25] T. Hahn, Comput. Phys. Commun. **140**, 418 (2001).
- [26] CTEQ Collaboration, H.L. Lai *et al.*, Eur. Phys. J. C **12**, 375(2000).
- [27] J. Pumplin et al J. High Energy Phys. **07** 012 (2002).
- [28] G. T. Bodwin, H. S. Chung, D. Kang, J. Lee and C. Yu, Phys. Rev. D **77** 094017 (2008).
- [29] K. T. Chao, Y. Q. Ma, H. S. Shao, K. Wang, and Y. J. Zhang, Phys. Rev. Lett. **108**, 242004 (2012).